Audio Engineering Society

Convention Paper 8921

Presented at the 134th Convention
2013 May 4–7 Rome, Italy

This Convention paper was selected based on a submitted abstract and 750-word precis that have been peer reviewed by at least two qualified anonymous reviewers. The complete manuscript was not peer reviewed. This convention paper has been reproduced from the author's advance manuscript without editing, corrections, or consideration by the Review Board. The AES takes no responsibility for the contents. Additional papers may be obtained by sending request and remittance to Audio Engineering Society, 60 East 42nd Street, New York, New York 10165-2520, USA; also see www.aes.org. All rights reserved. Reproduction of this paper, or any portion thereof, is not permitted without direct permission from the Journal of the Audio Engineering Society.

Wave Field Synthesis of Virtual Sound Sources with Axisymmetric Radiation Pattern Using a Planar Loudspeaker Array

Filippo Maria Fazi[1], Ferdinando Olivieri[1], Thibaut Carpentier[2], and Markus Noisternig[2]

[1] *Institute of Sound and Vibration Research, University of Southampton, University Road, SO17 1BJ Southampton, UK*

[2] *Acoustic and Cognitive Spaces Research Group, UMR STMS IRCAM-CNRS-UPMC, 1 place Igor-Stravinsky, 75004 Paris, France*

Correspondence should be addressed to Filippo Maria Fazi (ff1@isvr.soton.ac.uk)

ABSTRACT

A number of methods have been proposed for the application of Wave Field Synthesis to the reproduction of sound fields generated by point sources that exhibit a directional radiation pattern. However, a straightforward implementation of these solutions involves a large number of real-time operations that may lead to very high computational load. This paper proposes a simplified method to synthesize virtual sources with axisymmetric radiation patterns using a planar loudspeaker array. The proposed simplification relies on the symmetry of the virtual source radiation pattern and on the far-field approximation, although also a near-field formula is derived. The mathematical derivation of the method is presented and numerical simulations validate the theoretical results.

1. INTRODUCTION

Wave Field Synthesis (WFS) is a well-established sound reproduction technique that uses an array of loudspeakers, hereafter referred to as *secondary sources*, to recreate a certain sound field due to a *virtual acoustic source*. This technique was initially proposed by Berkhout in 1988 [1] and a number of later works, including for example references [2, 3, 4, 5], have proposed further improvements to this technique.

The operating principle of WFS relies on the so-called *Rayleigh's first integral formula* [6]. The latter

states that given a sound field $p(\mathbf{z})$ that is a solution of the homogeneous Helmholtz equation in the half-space $V \subset \mathbb{R}^3$, bounded by the infinite plane S, then

$$p\left(\mathbf{z}\right) = -2 \int_{\mathbf{x}\in S} \frac{e^{jk|\mathbf{z}-\mathbf{x}|}}{4\pi|\mathbf{z}-\mathbf{x}|} \frac{\partial p(\mathbf{x})}{\partial \mathbf{n}} dS, \quad \mathbf{z} \in V \qquad (1)$$

where $\mathbf{n}$ is a unitary vector normal to S and pointing towards the interior of V. This implies that the sound field p can be reproduced exactly in V by a continuous distribution of monopole sources, each of which is driven with a signal that is proportional to the value of the normal gradient of the target field evaluated at the source position. An approximate reproduction of the sound field can be achieved using a uniform planar array of loudspeakers.

In practical cases the reproduced field will not be an exact replica of the target because of the directional radiation patterns of the loudspeaker and especially because of the finite number of transducers. In fact, the finite extent of the array and the spacing between the loudspeakers are responsible of well-known reproduction artefacts, whose analysis is beyond the scope of this paper. In this work, a continuous planar distribution of ideal omnidirectional secondary sources is considered . It has to be mentioned, however, that most practical WFS systems rely on the use of linear loudspeaker arrays, for which a further operation is required, based on the stationary phase approximation [4].

Well-established examples of target sound fields include plane waves and the field due to an omnidirectional point source. For these cases, an analytical solution for the source signals is available [5]. More recently, solutions have been proposed also for a sound field due to point sources that exhibit a complex directivity pattern.

Corteel [7] proposed to synthesize directional sound sources using WFS by superposition of elementary directivity functions based on spherical harmonics (these functions are the elements of the series in equation (5) below). The formulation for the driving functions required for the synthesis of these elementary function relies on the far-field approximation of the spherical Hankel function, see also equation (8) below. In the same work, Corteel identified some limitations of this method and proposed an alternative approach based on the numerical solution of an inverse problem, whose implementation required the use of a bank of adaptive digital filters that are updated in real time.

Ahrens and Spors in [8] derived an expression for the loudspeaker driving signals for WFS of the sound field of a uniformly moving sound source with complex radiation properties. Also in this case a spherical harmonics description was adopted and the far-field approximation for the spherical Hankel functions was used. Despite this simplification, the resulting expression for the secondary source signals is quite complex because of the differentiation of the spherical harmonics.

Franck et al. in [9] have proposed an efficient signal processing method for rendering directional sources using time-frequency signal processing by using a fast convolution method which resulted in a significant reduction of the computational complexity. In this work the target field is described by a weighted series of circular harmonics and the far-field approximation of the Hankel functions is used.

In this work the closed-form expression is derived for the frequency-domain signals with which an infinite and continuous planar secondary source distribution is driven to reproduce (exactly) the sound field generated by a point source with an axisymmetric radiation pattern. With respect of existing approaches, the target sound field is simplified as it depends on one angular coordinate only. The usual spherical harmonic series reduces to a weighted sum of Legendre polynomials. The derivation is carried out without far-field approximation for the spherical Hankel function, thus obtaining a near-field expression for the driving functions.

The theoretical derivation, which consists of the analytical calculation of the normal gradient of the target sound field, is presented in Section 2. The results are validated by the numerical simulations reported in Section 3, which also emphasize the importance of the near-field formulation when very directive virtual sources are located in the vicinity of the secondary source array.

2. THEORETICAL MODEL

2.1. Reference geometry

The three orthogonal unitary vectors $\{\mathbf{u}_1, \mathbf{u}_2, \mathbf{u}_3\}$

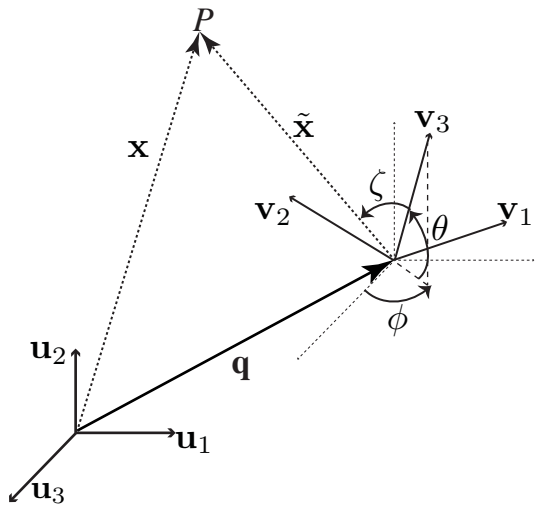

Fig. 1: Reference system

identify the primary Cartesian coordinate system, whilst $\{\mathbf{v}_1, \mathbf{v}_2, \mathbf{v}_3\}$ is a secondary reference system consistent with the virtual source as shown in Figure 1.

The axis of the virtual source is identified by $\mathbf{v}_3$, the loudspeaker array (secondary sources) lays on the plane spanned by $\mathbf{u}_1$ and $\mathbf{u}_2$ (vertical plane). The angle θ is the angle between $\mathbf{v}_3$ and the horizontal plane, spanned by $\mathbf{u}_1$ and $\mathbf{u}_3$, and the angle ϕ is the angle between $\mathbf{u}_3$ and the projection of $\mathbf{v}_3$ onto the horizontal plane.

Any vector $\mathbf{x}$ can be expressed as

$$\mathbf{x} = \sum_{i=1}^{3} x_i \mathbf{u}_i = \sum_{i=1}^{3} \tilde{x}_i \mathbf{v}_i + \mathbf{q} \tag{2}$$

where the vector $\mathbf{q}$ identifies the origin of the secondary reference system.

The following relations hold when the virtual source is located at the origin, i.e. $|\mathbf{q}| = 0$

$$\begin{aligned}
\mathbf{v}_1 &= \cos\phi \mathbf{u}_1 - \sin\phi \mathbf{u}_3 \\
\mathbf{v}_2 &= -\sin\theta \sin\phi \mathbf{u}_1 + \cos\theta \mathbf{u}_2 - \sin\theta \cos\phi \mathbf{u}_3 \\
\mathbf{v}_3 &= \cos\theta \sin\phi \mathbf{u}_1 + \sin\theta \mathbf{u}_2 + \cos\theta \cos\phi \mathbf{u}_3.
\end{aligned}$$

In this case, we have that the relation between the components $\mathbf{x} = [x_1, x_2, x_3]$ and $\tilde{\mathbf{x}} = [\tilde{x}_1, \tilde{x}_2, \tilde{x}_3]$ in the two reference systems, respectively, are related by the following formula

$$\tilde{\mathbf{x}} = \mathbf{R}\left(\mathbf{x} - \mathbf{q}\right) \tag{3}$$

The rotation matrix $\mathbf{R}$ is given by

$$\mathbf{R} = \begin{bmatrix} \cos\phi & 0 & -\sin\phi \\ -\sin\theta\sin\phi & \cos\theta & -\sin\theta\cos\phi \\ \cos\theta\sin\phi & \sin\theta & \cos\theta\cos\phi \end{bmatrix} \tag{4}$$

The spherical coordinates r, ζ, ξ of the secondary spherical coordinate system, consistent with the virtual source, are given by

$$\begin{aligned}
\tilde{x}_1 &= r\sin\zeta\cos\xi \\
\tilde{x}_2 &= r\sin\zeta\sin\xi \\
\tilde{x}_3 &= r\cos\zeta
\end{aligned}$$

where ζ is the angle between $\tilde{\mathbf{x}}$ and the vector $\mathbf{v}_3$, which identifies the axis of the virtual source.

2.2. Calculation of the secondary source driving functions

The target sound field generated by the virtual source can be expressed as a radiating solution of the Helmholtz equation. This can be expressed as [6]

$$p\left(r,\zeta,\xi,k\right) = \sum_{n=0}^{N}\sum_{m=-n}^{n} A_n^m\left(\omega\right) h_n\left(kr\right) Y_n^m\left(\zeta,\xi\right) \tag{5}$$

where $k = \frac{\omega}{c}$ is the wavenumber, c is the speed of sound, ω is the angular frequency, $j = \sqrt{-1}$ is the imaginary number, $h_n\left(kr\right)$ is the spherical Hankel function of the first kind and $Y_n^m\left(\zeta,\xi\right)$ are spherical harmonics [6]. It is assumed that the series above is limited to the finite order $N < \infty$.

For a virtual source with axisymmetric radiation pattern, with the symmetry axis identified by $\mathbf{v}_3$, the sound field $p\left(r,\zeta,\xi,k\right)$ does not depend on the angular coordinate ξ. In this case all the coefficients $A_n^m\left(\omega\right)$ with $m \neq 0$ are zero and the expression above can be simplified as

$$p\left(r,\zeta,k\right) = \frac{jk}{4\pi}\sum_{n=0}^{N} B_n\left(\omega\right) j^n h_n\left(kr\right) P_n\left(\cos\zeta\right) \tag{6}$$

where

$$B_n(\omega) := \frac{\sqrt{4\pi(2n+1)}}{j^{n+1}k} A_n^0(\omega) \tag{7}$$

and $P_n(\cos\zeta)$ are the Legendre polynomials of degree n [6].

The far-field radiation pattern $D(\zeta,\omega)$ can be derived in view of the large argument approximation of the Hankel functions [6]

$$h_n(x) \approx j^{-n}\frac{e^{jx}}{jx} \tag{8}$$

and is given by

$$D(\zeta,\omega) = \sum_{n=0}^{N} B_n(\omega) P_n(\cos\zeta) \tag{9}$$

Multiplying both sides of this equation by a Legendre polynomial of arbitrary order, integrating over a semicircle and applying the orthogonality of the Legendre polynomials in the interval $[-1,1]$ [6] yields

$$B_n(\omega) = \frac{2}{2n+1}\int_0^{\pi} D(\zeta,\omega) P_n(\cos\zeta)\sin\zeta d\zeta \tag{10}$$

The normal derivative of the sound field p is given by [6]

$$\frac{\partial p(r,\zeta,k)}{\partial \mathbf{n}} = \mathbf{n}\cdot\nabla p(r,\zeta,k) = \mathbf{n}\cdot\mathbf{R}^T\tilde{\nabla} p(r,\zeta,k)$$
$$= \mathbf{R}\mathbf{n}\cdot\left[\tilde{\mathbf{r}}\frac{\partial}{\partial r} + \frac{\tilde{\mathbf{b}}}{r}\frac{\partial}{\partial\zeta} + \frac{\tilde{\mathbf{d}}}{r\sin\zeta}\frac{\partial}{\partial\xi}\right] p(r,\zeta,k) \tag{11}$$

where

$$\tilde{\nabla} := \sum_{i=1}^{3}\mathbf{v}_i\frac{\partial}{\partial\mathbf{v}_i} \tag{12}$$

$$\tilde{\mathbf{r}} := \tilde{\nabla} r$$
$$= \sin\zeta\cos\xi\mathbf{v}_1 + \sin\zeta\sin\xi\mathbf{v}_2 + \cos\zeta\mathbf{v}_3 \tag{13}$$

$$\tilde{\mathbf{b}} := \tilde{\nabla}\zeta$$
$$= \cos\zeta\cos\xi\mathbf{v}_1 + \cos\zeta\sin\xi\mathbf{v}_2 - \sin\zeta\mathbf{v}_3 \tag{14}$$

$$\tilde{\mathbf{d}} := \tilde{\nabla}\xi = -\sin\xi\mathbf{v}_1 + \cos\xi\mathbf{v}_2 \tag{15}$$

The following relations are used to compute the derivative of the spherical Hankel functions [10, p. 925], [6, p.197] and for the Legendre polynomials and associated functions [6, p. 188], [10, p. 965]:

$$h_n(kr) = j^{-n}h_0(kr)\sum_{\alpha=0}^{n}\frac{\tau_{n,\alpha}}{(jkr)^{\alpha}} \tag{16}$$

$$\tau_{n,\alpha} = (-1)^{\alpha}\frac{(n+\alpha)!}{\alpha!(n-\alpha)!2^{\alpha}} \tag{17}$$

$$\frac{\partial h_n(kr)}{\partial kr} = \frac{n}{kr}h_n(kr) - h_{n+1}(kr) \tag{18}$$

$$\frac{dP_n(\cos\zeta)}{d\zeta} = -\sin\zeta\frac{dP_n(\cos\zeta)}{d\cos\zeta}$$
$$= -n(n+1)P_n^{-1}(\cos\zeta) \tag{19}$$

$$P_n^{-1}(\cos\zeta) = -\frac{(n-1)!}{(n+1)!}P_n^1(\cos\zeta)$$
$$= -\frac{1}{n(n+1)}P_n^1(\cos\zeta) \tag{20}$$

These formulae yield

$$\frac{\partial h_n(kr)}{\partial kr} = h_0(kr)\,j^{-n}\sum_{\alpha=0}^{n+1}\frac{j}{(jkr)^{\alpha}}$$
$$\times\left[\tau_{n+1,\alpha} + \tau_{n,\alpha}\frac{n}{jkr}(1-\delta_{\alpha,n+1})\right]$$
$$= h_0(kr)\,j^{1-n}\left[1 + \sum_{\alpha=0}^{n}\frac{\tau_{n,\alpha}\sigma_{n,\alpha}}{(jkr)^{\alpha+1}}\right] \tag{21}$$

with $\delta_{n,\alpha}$ being the Kronecker delta and

$$\sigma_{n,\alpha} := \left[n - \frac{(n+\alpha+1)(n+\alpha+2)}{2(\alpha+1)}\right]$$
$$= -\frac{n^2+\alpha^2+3\alpha+n+2}{2(\alpha+1)} \tag{22}$$

and

$$\frac{dP_n(\cos\zeta)}{d\zeta} = P_n^1(\cos\zeta). \tag{23}$$

In the light of these results, the sound field derivatives are calculated with respect to the radial coordinate r

$$\frac{\partial p(r,\zeta,k)}{\partial r} = \frac{jk}{4\pi}\sum_{n=0}^{N}B_n(\omega)\,j^n P_n(\cos\zeta)\,k\frac{\partial h_n(kr)}{\partial kr}$$
$$= h_0(kr)\,\frac{jk}{4\pi}\sum_{n=0}^{N}B_n(\omega)\,j^n P_n(\cos\zeta)$$
$$\times\left[jk + \frac{1}{r}\sum_{\alpha=0}^{n}\frac{\tau_{n,\alpha}\sigma_{n,\alpha}}{(jkr)^{\alpha}}\right] \tag{24}$$

and the angular coordinate ζ

$$\frac{\partial p\left(r,\zeta,k\right)}{\partial\zeta}=\frac{jk}{4\pi}\sum_{n=0}^{N}B_n\left(\omega\right)j^n h_n\left(kr\right)\frac{\partial P_n\left(\cos\zeta\right)}{\partial\zeta}$$
$$=\frac{jk}{4\pi}h_0\left(kr\right)\sum_{n=1}^{N}B_n\left(\omega\right)P_n^1\left(\cos\zeta\right)\sum_{\alpha=0}^{n}\frac{\tau_{n,\alpha}}{(jkr)^\alpha}. \quad (25)$$

Clearly, the derivative with respect to the second angular coordinate ξ is zero.

Substituting the results obtained in equations (24) and (25) into equation (11) yields

$$\frac{\partial p}{\partial\mathbf{n}}=\mathbf{Rn}\cdot\tilde{\mathbf{r}}\frac{\partial p}{\partial r}+\frac{1}{r}\mathbf{Rn}\cdot\tilde{\mathbf{b}}\frac{\partial p}{\partial\zeta}$$
$$=\frac{\exp\left(jkr\right)}{4\pi r}\sum_{n=0}^{N}B_n\left(\omega\right)$$
$$\times\left\{\mathbf{Rn}\cdot\tilde{\mathbf{r}}P_n\left(\cos\zeta\right)\left[jk+\frac{1}{r}\sum_{\alpha=0}^{n}\frac{\sigma_{n,\alpha}\tau_{n,\alpha}}{(jkr)^\alpha}\right]\right.$$
$$\left.+\frac{1}{r}\mathbf{Rn}\cdot\tilde{\mathbf{b}}P_n^1\left(\cos\zeta\right)\left(1-\delta_{n,0}\right)\sum_{\alpha=0}^{n}\frac{\tau_{n,\alpha}}{(jkr)^\alpha}\right\} \quad (26)$$

Hence, the frequency-domain driving signal $w_\ell\left(\omega\right)$ for a secondary source (loudspeaker) located at $[r_\ell,\zeta_\ell,\xi_\ell]$ (with respect to the secondary coordinate system) is obtained by substituting equation (26) into equation (1), thus obtaining

$$w_\ell\left(\omega\right)=-2\frac{\partial p\left(r_\ell,\zeta_\ell,k\right)}{\partial\mathbf{n}}$$
$$=-2\frac{\exp\left(jkr_\ell\right)}{4\pi r_\ell}\sum_{n=0}^{N}B_n\left(\omega\right)$$
$$\times\left\{jk\mathbf{Rn}\cdot\tilde{\mathbf{r}}_\ell P_n\left(\cos\zeta_\ell\right)+\frac{1}{r_\ell}\sum_{\alpha=0}^{n}\frac{\tau_{n,\alpha}}{(jkr_\ell)^\alpha}\right.$$
$$\times\left[\mathbf{Rn}\cdot\tilde{\mathbf{r}}_\ell P_n\left(\cos\zeta_\ell\right)\sigma_{n,\alpha}\right.$$
$$\left.\left.+\mathbf{Rn}\cdot\tilde{\mathbf{b}}_\ell P_n^1\left(\cos\zeta_\ell\right)\left(1-\delta_{n,0}\right)\right]\right\} \quad (27)$$

or equivalently

$$w_\ell\left(\omega\right)=-2\frac{\partial p\left(r_\ell,\zeta_\ell,k\right)}{\partial\mathbf{n}}$$
$$=-2\frac{\exp\left(jkr_\ell\right)}{4\pi r_\ell}\left\{\mathbf{Rn}\cdot\tilde{\mathbf{r}}_\ell\sum_{n=0}^{N}B_n\left(\omega\right)P_n\left(\cos\zeta_\ell\right)\right.$$
$$\times\left[jk+\frac{1}{r_\ell}\sum_{\alpha=0}^{n}\frac{\sigma_{n,\alpha}\tau_{n,\alpha}}{(jkr)^\alpha}\right]$$
$$\left.+\mathbf{Rn}\cdot\tilde{\mathbf{b}}_\ell\sum_{n=1}^{N}B_n\left(\omega\right)P_n^1\left(\cos\zeta_\ell\right)\frac{1}{r_\ell}\sum_{\alpha=1}^{n}\frac{\tau_{n,\alpha}}{(jkr)^\alpha}\right\} \quad (28)$$

The WFS formulation in equation (28) is hereafter referred to as the *near-field formulation*.

2.3. Far-field approximation

By neglecting in equation (28) all terms whose amplitude decays with distance faster than $1/r$ it is possible to obtain the *far-field approximation* of the secondary source signals, that is

$$w_\ell^{FF}\left(\omega\right)=-2\frac{\partial p_{FF}\left(r_\ell,\zeta_\ell,k\right)}{\partial\mathbf{n}}$$
$$=-2jk\frac{\exp\left(jkr_\ell\right)}{4\pi r_\ell}\mathbf{Rn}\cdot\tilde{\mathbf{r}}_\ell\sum_{n=0}^{N}B_n\left(\omega\right)P_n\left(\cos\zeta_\ell\right) \quad (29)$$

3. SIMULATIONS

The aim of the numerical simulations presented in this section is to evaluate the performances of the proposed method. It highlights the advantage of using the near-field formulation for the WFS of sources located in the near-field of the secondary source distribution.

Hereafter, the sound field due to the virtual sound source is referred to as the *target sound field* and it is indicated by $p_{\text{target}}(\mathbf{x})$, whilst the sound field due to the secondary sources is referred to as the *reconstructed sound field* and is indicated by $p_{\text{reconstr}}(\mathbf{x})$. Furthermore, the two different formulations for the secondary source signals presented in equations (28) and (29) are referred to as the *near-field formulation* and *far-field approximation*, respectively.

3.1. Geometry

The three dimensional volume considered in all the simulations is a square box A of volume

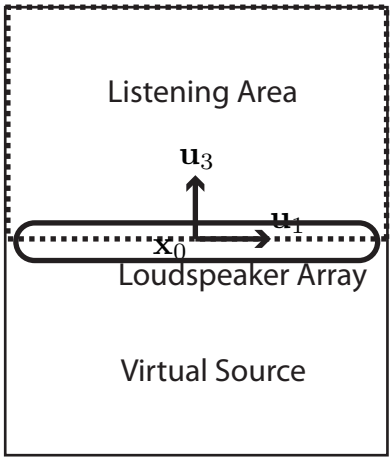

Fig. 2: Volume A as seen from above.

$[5 \times 5 \times 5]$ m^3 in which the speed of sound is assumed to be uniformly equal to $c = 343$ m/s.

The origin of the primary reference system is $\mathbf{x}_0 = [0, 0, 0]$ and is located in the middle of the volume A. The listening area is located in the part of the 3D space where x_3 has positive values, whilst the virtual source is located in the portion of the space where x_3 is negative. Figure 2 provides a diagrammatic representation of the volume A as seen from above. The listening area, a portion of the loudspeaker array, and the region where the virtual source may be located are indicated.

The loudspeaker array is planar and lies on the plane spanned by $\mathbf{u}_1$ and $\mathbf{u}_2$, thus dividing the volume A in two parts (the listening region and the virtual sound source region). The loudspeakers are arranged in a regular, squared lattice of 175×175 units. The spacing between loudspeaker is $d = \lambda/12$, where $\lambda = c/f_0$ is the wave length of the monochromatic sound to be reproduced.

3.2. Virtual sources

The virtual sources being considered are time-harmonic sound sources operating at frequency $f_0 = 500$ Hz with two different radiation patterns: a dipole and a quadrupole. In both cases, the virtual sources have unitary source strength.

As mentioned in section 3.1, the virtual source is located behind the wall of loudspeakers. Two different virtual source positions are considered: in the far-field, at $\mathbf{q}_1 = [0, 0, -4\lambda]$, and in the near-field, at $\mathbf{q}_2 = [0, 0, -\lambda]$.

For the virtual source (and for each given radiation pattern) located at $\mathbf{q}_1$ only the far-field formulation is used for the WFS of the target sound field. In the case of the virtual source located at $\mathbf{q}_2$ both the far-field approximation and the near-field formulation are used in order to demonstrate their different performance.

3.3. Evaluation of performances

The reproduction performance has been evaluated by calculating the amplitude and phase errors between the target and the reconstructed sound fields. The amplitude error is defined as

$$\epsilon_{\text{amp}} = 10 \log_{10} \left[\frac{|p_{\text{reconstr}}(\mathbf{x})|^2}{|p_{\text{target}}(\mathbf{x})|^2} \right] \tag{30}$$

whilst the phase error is defined as

$$\epsilon_{\text{phase}} = \angle \left[p_{\text{reconstr}}(\mathbf{x}) p_{\text{target}}(\mathbf{x})^* \right] \tag{31}$$

These two errors and the target and reconstructed sound fields in the plane spanned by $\mathbf{u}_1$ and $\mathbf{u}_3$ are presented in what follows.

3.4. Dipole-like virtual source

The series coefficients for this examples are $B_n(\omega) = \delta_{n,1}$, where δ represents the Kronecker delta. This implies that only the coefficient with $n = 1$ is different from zero. Figure 3 shows the target and reconstructed fields of a dipole source located in the far field at $\mathbf{q}_1$ and rotated by $\phi = 45°$ as well as the amplitude and phase errors.

The presence of reproduction artefacts can be observed. The amplitude and phase errors are, however, quite small, apart from the nodal line of the dipole field, where the pressure is zero.

The sound fields and reproduction errors for the near-field case are reported in figures 4 and 5, computed using the far-field approximation and the near-field formulation, respectively. It can be clearly seen that in this case the far-field approximation creates significant reproduction errors, especially for the amplitude. Note that this error is not restricted to the near-field of the loudspeaker array. As expected, for the near-field formulation this error is dramatically reduced.

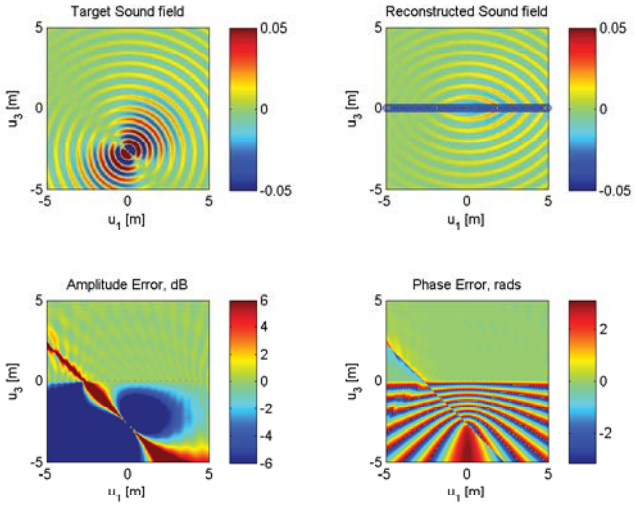

Fig. 3: Dipole source located in the far-field at $\mathbf{q}_1$. Synthesis performed with the far-field formulation.

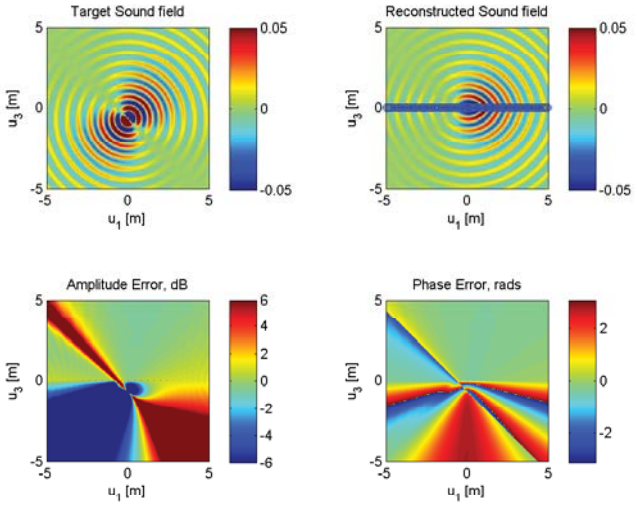

Fig. 4: Dipole source located in the near-field at $\mathbf{q}_2$. Synthesis performed with the far-field formulation.

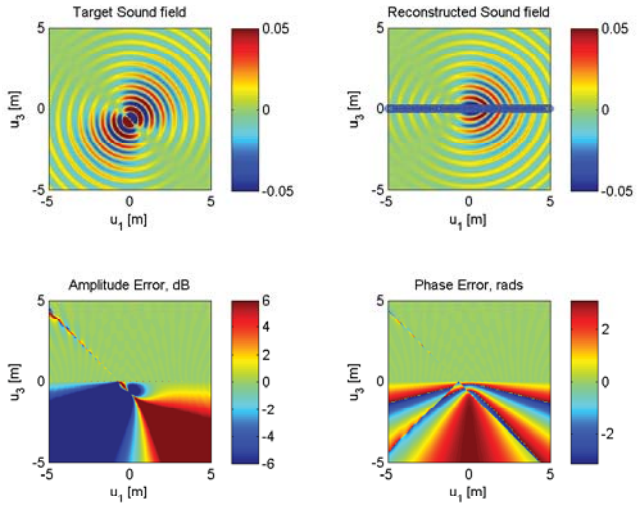

Fig. 5: Dipole source located in the near-field at $\mathbf{q}_2$. Synthesis performed with the near-field formulation.

3.5. Quadrupole-like virtual source

The series coefficients for this example are $B_n(\omega) = \delta_{n,2}$. Figure 6 shows the target and reconstructed fields when the virtual source is located in the far field at $\mathbf{q}_1$ and rotated by $\phi = 45°$, as well as the amplitude and phase errors. The far-field formulation was used for the secondary source signals. As in the previous example, the reproductions errors are small, with the exception of the nodal line of the quadrupole field

The results of the WFS of the quadrupole source located at position $\mathbf{q}_2$ using the far-field approximation and the near-field formulation are shown in Figure 7 and Figure 8, respectively. As in the dipole example, the far-field approximation generates significant reproduction error, which extends beyond the near-field of the array, whilst this is not the case when the secondary source signals were calculated with the near-field formulation.

4. CONCLUSION

A closed-form expression has been derived, in the frequency domain, for the signals with which an infinite, planar array of secondary sources may be driven in order to reproduce the sound field due to a virtual source with axisymmetric radiation pattern. The solution was derived taking into consideration the near-field components of the target field.

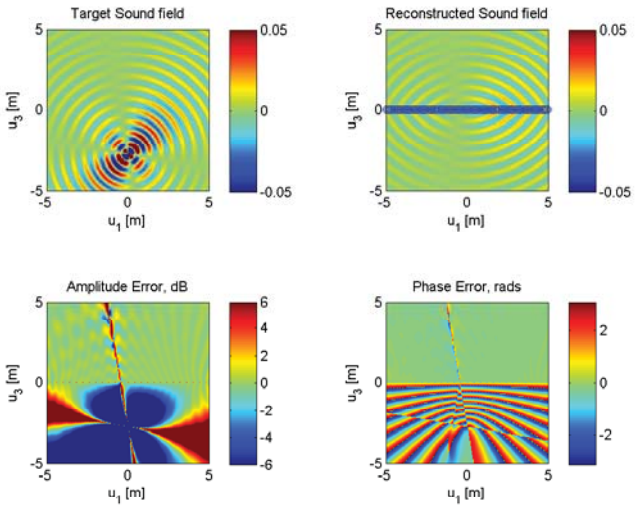

Fig. 6: Quadrupole source located in the far-field at $\mathbf{q}_1$. Synthesis performed with the far-field formulation.

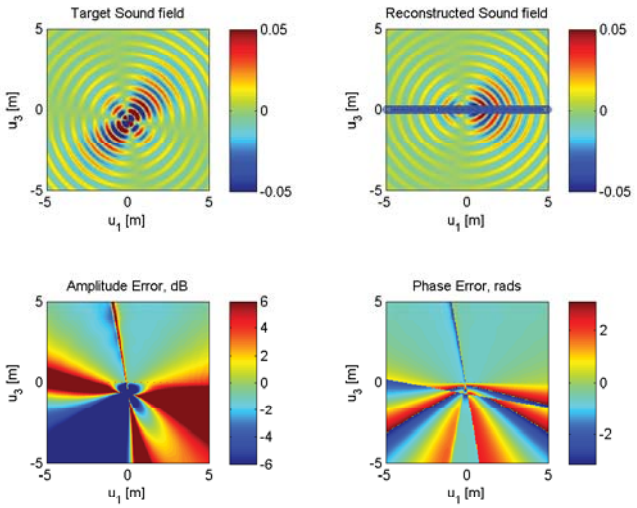

Fig. 7: Quadrupole source located in the near-field at $\mathbf{q}_2$. Synthesis performed with the far-field formulation.

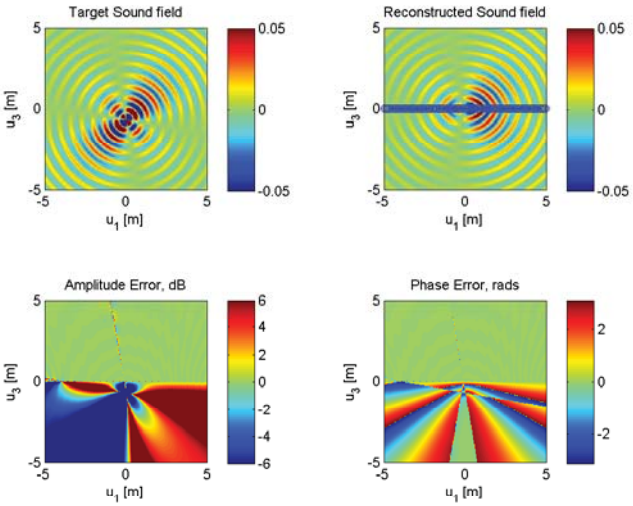

Fig. 8: Quadrupole source located in the near-field at $\mathbf{q}_2$. Synthesis performed with the near-field formulation.

A far-field formulation has also been proposed, which has been derived by neglecting the components of the sound field whose amplitude decays more rapidly than $1/r$. In comparison to other approaches reported in the literature, the proposed far-field method is very simple and seems to be optimally suited for real-time implementation.

Numerical simulations have demonstrated that, when the virtual source is located in the vicinity of the secondary source distribution and the far-field approximation is used to compute the driving signals, a significant reproduction error is generated, which may extends beyond the near-field of the array. This problem has been overcome using the near-field formulation.

Future work may include time domain derivation of the secondary source signals (with near-field formulation), as well as the design and realization of the DSP implementation of the proposed method. Finally, the effectiveness of the techniques presented may be tested also for the case of focused sources, that is virtual sources that are located in the region of the space between the listener and the secondary source distribution.

5. ACKNOWLEDGEMENTS

This project was funded in part by the French ANR CONTINT project "Sample Orchestrator 2" (SOR2), by the Royal Academy of Engineering, and by the Engineering and Physical Sciences Research Council, UK.

6. REFERENCES

[1] A. J. Berkhout, "A Holographic Approach to Acoustic Control", *J. Audio. Eng. Soc.*, vol. 36, no. 12, pp. 977-9950, 1988

[2] A. J. Berkhout, D. Devries, and P. Vogel, "Acoustic Control by Wave Field Synthesis", *J. Acoust. Soc. Am.*, vol. 93, no. 5, pp. 2764-2778, 1993

[3] E. N. G. Verheijen, *Sound Reproduction by Wave Field Synthesis*, Delft University of Technology, PhD thesis, 1997

[4] E. W. Start, *Direct Sound Enhancement by Wave Field Synthesis*, Delft University of Technology, PhD thesis, 1997

[5] S. Spors, R. Rabenstein, and J. Ahrens, "The Theory of Wave Field Synthesis Revisited", presented at the *124th Conv. of the Audio Eng. Soc.*, Amsterdam, The Netherlands, 2008

[6] E. G. Williams, *Fourier acoustics: sound radiation and nearfield acoustical holography*, Academic Press, San Diego, 1999.

[7] E. Corteel, "Synthesis of directional sources using wave field synthesis, possibilities, and limitations", *EURASIP J. on Advances in Signal Process.*, Vol. 2007, 2007.

[8] J. Ahrens and S. Spors, "Wave field synthesis of moving virtual sound sources with complex radiation properties", *J. Acoust. Soc. Am.*, Vol. 130 n. 5, pp 2807-2816.

[9] A. Franck, M. Rath, C. Sladeczek, and S. Brix, " Efficient Rendering of Directional Sound Sources in Wave Field Synthesis", presented at the *45th Int. Conf. of the Audio Eng. Soc.*, Helsinki, Finland, 2012 March 14.

[10] I. S. Gradshteyn and I. M. Ryzhik, *Table of integrals, series and products*, Academic Press, New York, 1965.